Available online at www.sciencedirect.com
ScienceDirect
Materials Chemistry and Physics 103 (2007) 394–399
MATERIALS CHEMISTRY AND PHYSICS
www.elsevier.com/locate/matchemphys

# Structural characterization of phase transition of $Al_2O_3$ nanopowders obtained by polymeric precursor method

S. Cava [a,*], S.M. Tebcherani [a], I.A. Souza [b], S.A. Pianaro [a], C.A. Paskocimas [c], E. Longo [b], J.A. Varela [b]

[a] *Laboratório Interdisciplinar de Materiais Cerâmicos, Centro Interdisciplinar de Pesquisa e Pós-Graduação, Universidade Estadual de Ponta Grossa, Av. Gal. Carlos Cavalcanti, 4748, Campus-Uvaranas, CEP 84035-900, Ponta Grossa, PR, Brazil*

[b] *Laboratório Interdisciplinar em Cerâmica, Departamento de Físico-Química, Instituto de Química, Universidade Estadual Paulista, R. Francisco Degni, s/n, Bairro Quitandinha, Araraquara, SP, Brazil*

[c] *Departamento de Engenharia Mecânica, Universidade Federal do Rio Grande do Norte, Campus Universitário, S/N, Lagoa Nova, CEP 59072-970, Natal, RN, Brazil*

Received 5 August 2005; received in revised form 19 April 2006; accepted 18 February 2007

**Abstract**

Nanocrystalline $Al_2O_3$powders have been synthesized by the polymeric precursor method. A study of the evolution of crystalline phases of obtained powders was accomplished through X-ray diffraction, micro-Raman spectroscopy and refinement of the structures through the Rietveld method. The results obtained allow the identification of three steps on the γ-$Al_2O_3$ to α-$Al_2O_3$ phase transition. The single-phase α-$Al_2O_3$ powder was obtained after heat-treatment at 1050 ° C for 2 h. A study of the morphology of the particles was accomplished through measures of crystallite size, specific surface area and transmission electronic microscopy. The particle size is closely related to γ-$Al_2O_3$ to α-$Al_2O_3$ phase transition.


*Keywords:* $Al_2O_3$; Phase transition; Polymeric precursor method; Nanopowders; Micro-Raman spectroscopy; Crystallite size

## 1. Introduction

Ultrafine and nanosized single-metal oxide powders have been given a lot of attention as a possibility for functional materials of electrical parts and structural materials of mechanical parts [1]. Currently and for the foreseeable future, the most important types of nanoparticles are simple oxides, such as $Al_2O_3$, used in established applications [2,3]. During sintering and shaping of oxidic materials for practical applications, use of nano sized particles as starting materials can be of great advantage because of the availability of large surface areas of the nanoparticles [4].

Conventional methods for synthesizing α-$Al_2O_3$powder involve solid state thermally driven transformations from the hydrates of aluminium oxide. The extent of conversion to the corundum structure depends on the temperature and the time of thermal treatment. Total conversion occurs on heating above 1230 ° C [5].

We have previously described the use of polymeric precursor method as a means of producing alumina powders and influence of cobalt in the formation of α-$Al_2O_3$at around 1050 ° C [6]. In addition, the influence of cobalt localization in spectroscopic transitions of alumina phases was evaluated. On the other hand, the influence of particle size was not investigated.

In this way, the object of this study is to evaluate the particle size of $Al_2O_3$nanopowders prepared by means of polymeric precursor method and to study the relationship between phase transition.

## 2. Experimental procedure

Preparations used alumina nanoparticles that had been synthesized by means of polymeric precursor method in experiments that will be described in more detail elsewhere [6]. Summarizing, ammonium alum – $NH_4Al(SO_4)_2$was first dissolved in distilled water and ammonium hydroxide – $NH_4OH$ in order to form aluminum hydroxide – $Al(OH)_3$. With addition of citric acid anhydrous – $C_6H_8O_7$, the formation of aluminum citrate takes place. The polymerization occurred upon the addi-

* Corresponding author. Tel.: +55 42 2203055; fax: +55 42 2203150.
*E-mail address:* cava@uepg.br (S. Cava).

0254-0584/$ – see front matter © 2007 Elsevier B.V. All rights reserved.
doi:10.1016/j.matchemphys.2007.02.046

tion of ethylene glycol – $C_2H_6O_2$. The heat-treatment of the resin was made in an air atmosphere in an oven at 400 ° C for 1 h, in order to burn the organic matter that became a black solid mass. This mass was finely ground in an Attritor mill for 1 h. The powder obtained was heat-treated in an oxygen atmosphere at 500 ° C for 4 h, in order to oxidate the remaining organic matter. In the furnace, the precursor was heat-treated at the 700–1200 ° C range in air, in an $Al_2O_3$boat, and then cooled to room temperature.

The determination of the crystalline phases and the cell volume was carried out, using $SiO_2$ as an external standard, by X-ray diffraction (XRD) patterns, which were obtained with a Siemens D-5000 diffractometer with Cu K α radiation (λ = 1.5406 Å and $\theta$ =20–75°), at room temperature. The average crystallite size of obtained powders was estimated by Scherrer's equation from the XRD pattern and also observed by transmission electronic microscopy (TEM) employing a Philips CM200 equipment.

For the refinement and micro-structural analysis, the GSAS [7] program was used based on the Rietveld method, and the function profile chosen was the pseudo-Voigt [8–10], which allows a good adjustment in order to accentuate asymmetries of the profile at low angles.

Raman spectra were performed in these samples. The excitation was at the 514.5 nm line of an argon ion laser, with 15 mW power, and using a 50×lens. The backscattering geometry was applied for detection.

The surface area measurements of the powders were accomplished in a Micrometrics, ASAP 2000 equipment, using $N_2$ as the adsorption/desorption gas. The mean diameter obtained by

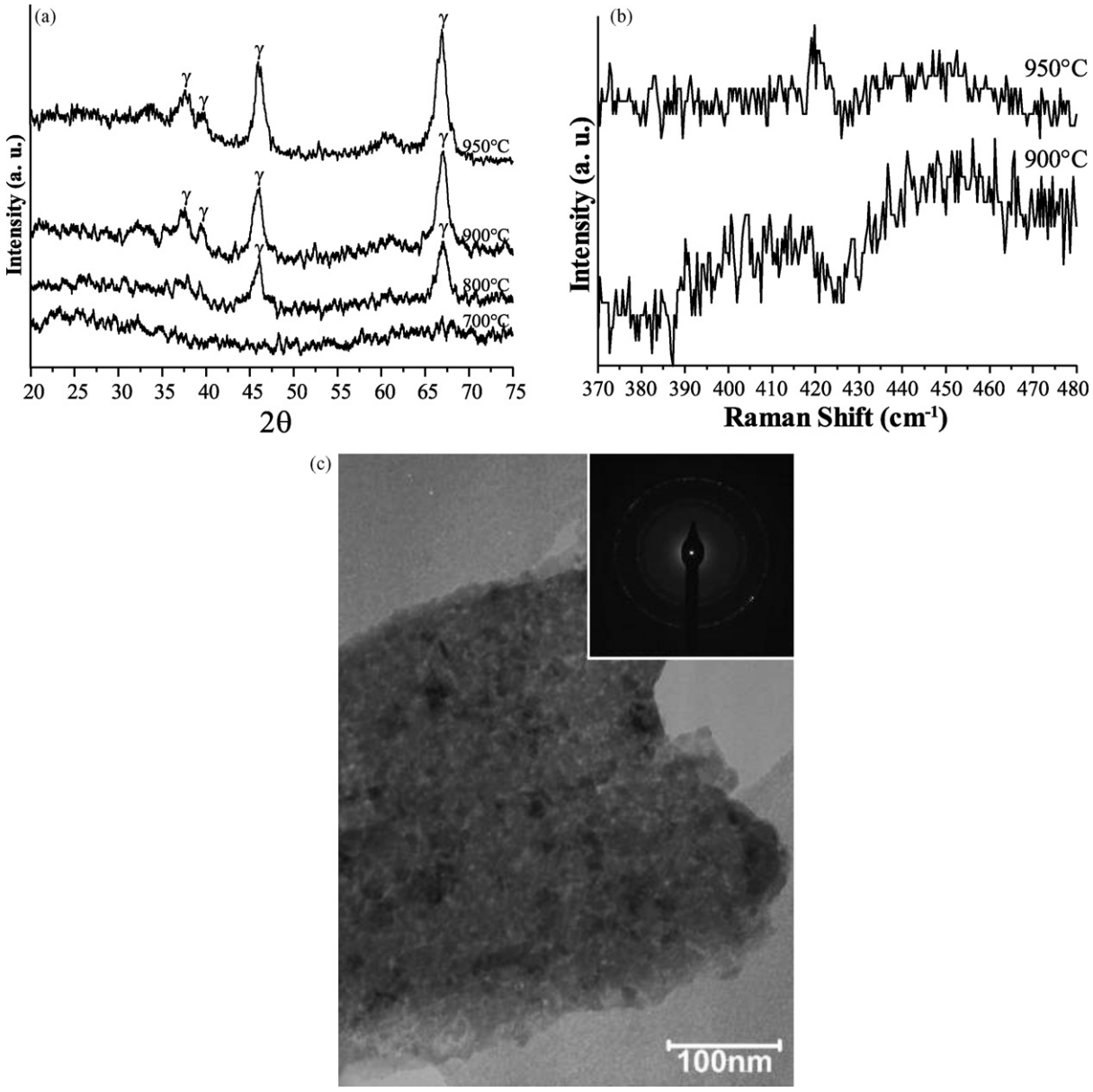


Fig. 1. Characterization of γ-$Al_2O_3$ powders γ-$Al_2O_3$: (a) XRD diffraction patterns; (b) micro-Raman spectra; (c) TEM micrographs of the sample at 950 °C.

applying the BET method, $d_{BET}$, is represented by

$$d_{BET} = \frac{6}{A_s \rho} \quad (1)$$

where $A_s$ is the specific surface area ($m^2\,g^{-1}$) and $\rho$ is the theoretical density of the phase ($\rho_{Al_2O_3} = 3.9\,g\,cm^{-3}$).

## 3. Results and discussion

Figs. 1–3 display the diffraction patterns, micro-Raman spectroscopy and transmission electronic micrographs of the $Al_2O_3$ system in three steps of phase transition.

The first step is the presence of single phase γ-$Al_2O_3$ (Fig. 1).

The second step is the phase transition with the presence of both γ-$Al_2O_3$ and α-$Al_2O_3$ phase (Fig. 2).

The third step is the presence of single phase α-$Al_2O_3$ (Fig. 3).

As indicated by Fig. 1(a), at temperatures up to 700 °C, the patterns are ascribed to an amorphous phase.

Between 800 and 900 °C, progressive dehydration and desorption of surface hydroxyl groups lead to the formation of the γ-$Al_2O_3$. This phase is based on a distorted spinel structure [11]. While most of the features could be accounted for by the fit, the peaks exhibit broad and diffuse profiles, indicating the presence of small crystalline grains and compositional fluctuations. This is consistent with the location of the $Al^{3+}$ions either by the tetrahedral or octahedral sites within the spinel structure.

Fig. 1(b) displays micro-Raman spectra for temperature range of 900–950 °C, in that there is not sign, due to the cubic symmetry of the γ-$Al_2O_3$, demonstrating absence of α-$Al_2O_3$(hexagonal symmetry).

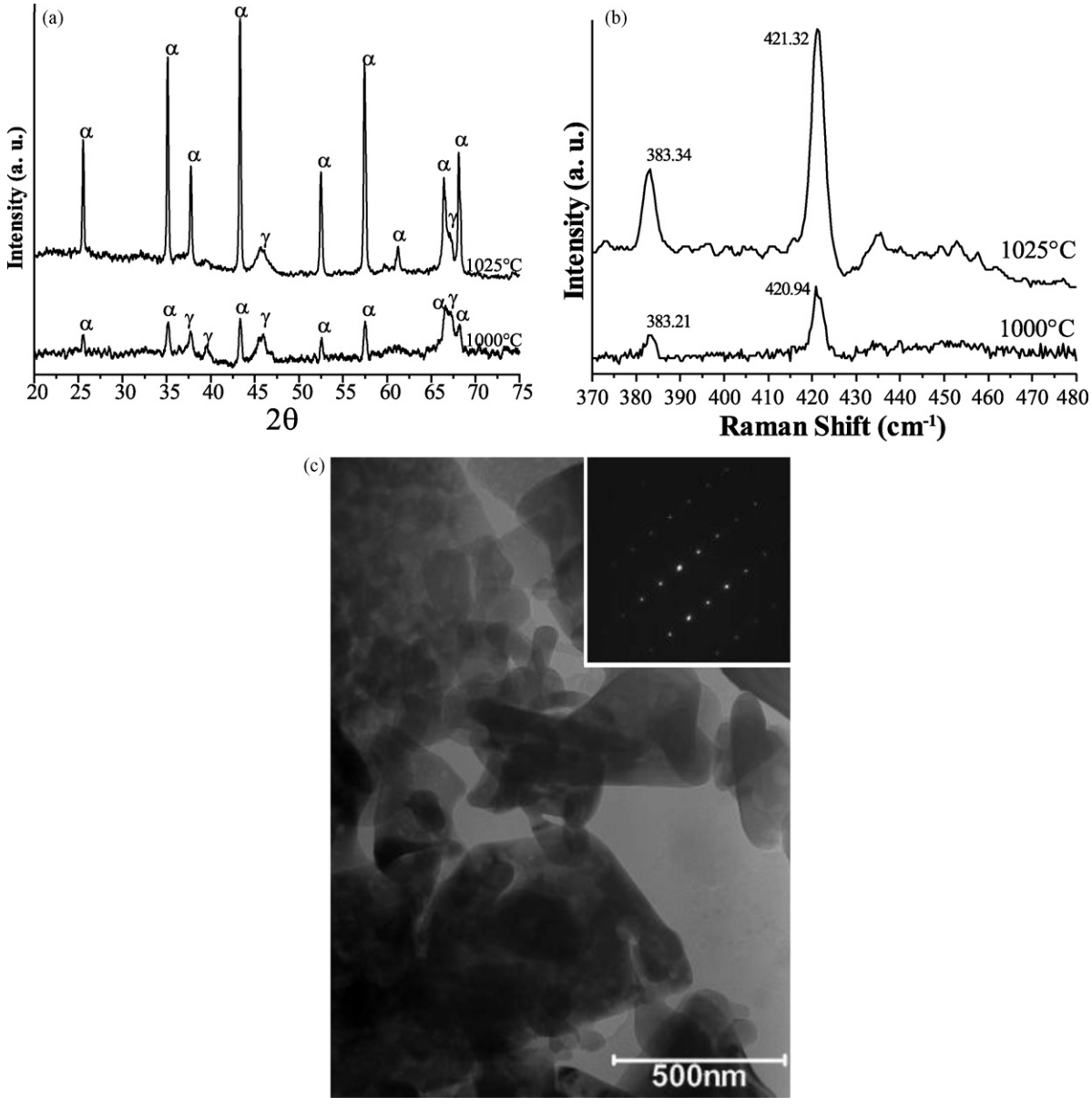


Fig. 2. Characterization of powders in the temperature range of phase transition, containing γ-$Al_2O_3$ and α-$Al_2O_3$: (a) XRD diffraction patterns; (b) micro-Raman spectra; (c) TEM micrographs of the sample at 1025 °C.

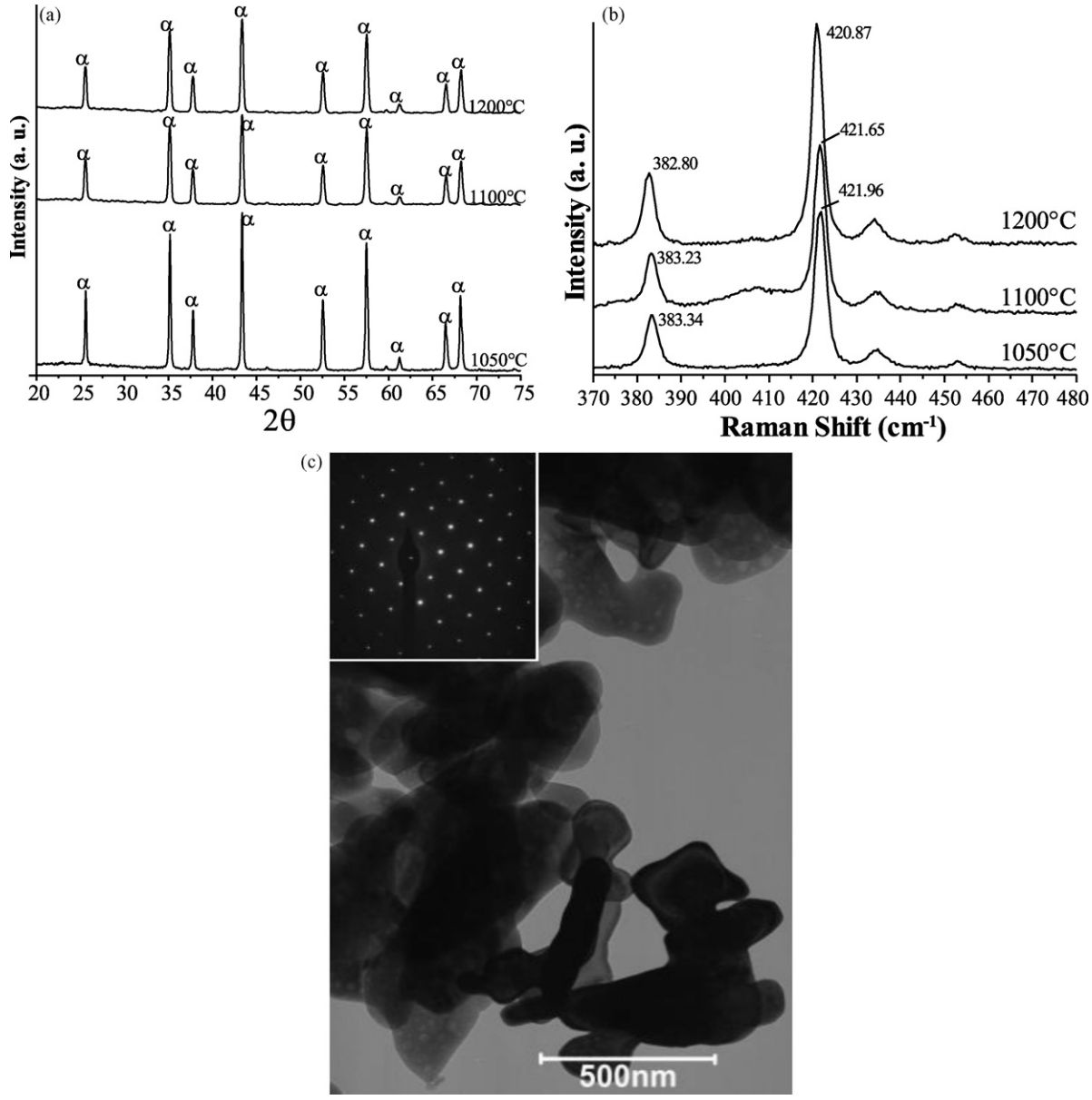


Fig. 3. Characterization of γ-$Al_2O_3$ powders: (a) XRD diffraction patterns; (b) micro-Raman spectra; (c) TEM micrographs of the sample at 1050 °C.

At 1000 and 1025 ° C (Fig. 2(a)), the occurrence of additional peaks in X-ray patterns became evident, indicating the co-existence of the γ-$Al_2O_3$and α-$Al_2O_3$phases, as confirmed by micro-Raman spectra in Fig. 2(b), with characteristics peaks at 380 and 420 $cm^{-1}$.

Transformation of all pure alumina into the single α-phase was observed starting from 1050 °C, as indicated by Fig. 3(a) and (b). The sharp peaks of the α-phase indicate the relatively large grain sizes and well-defined long-range order in corundum, which signifies the collapse of the porous structure characteristic of the low-temperature phases and the consequent diminishment of the powder surface area.

Peaks due to γ-$Al_2O_3$disappear when the temperature is higher to 1050 °C, forming the α-$Al_2O_3$. The powders do not present any impurities, due to incomplete transformations of any intermediate phases, as θ and δ, as it happens in conventional methods of processing [12].

Usually, by means of traditional methods of synthesis, any aluminum oxide or hydroxide only form α-$Al_2O_3$when the material is fired up to 1200 ° C [13]. In the present work, the formation of the α-$Al_2O_3$at 1050 ° C was obtained, due to the polymeric precursor method used. By means of this method it is possible to obtain materials with lower calcination temperatures, due to the chemical method of interaction between the network former cations.

Refinements of Rietveld method were performed by means of GSAS (generalized structure analysis system) [7] from crystallographic data of γ-$Al_2O_3$[11] and α-$Al_2O_3$[14,15] and XRD diffraction patterns data samples calcined at 950, 1025 and 1050 °C. The obtained results are presented in Table 1.

Table 1
Results from Rietveld refinement of the samples calcined at 950, 1025 and 1050 °C

| | Temperature (°C) | | | |
|---|---|---|---|---|
| | 950 | 1025 | | 1050 |
| | 100% γ [a] | 46.6% γ [a] | 53.4% α [a] | 100% α [a] |
| $a = b$ | 7.95 | 8.08 | 4.76 | 4.76 |
| $c$ | 7.95 | 8.08 | 12.99 | 12.99 |
| $\chi^2$ | 2.89 | 5.85 | | 1.67 |

[a] Phase.

The existence of a critical temperature of phase transition is observed between 1000 and 1050 °C, where there is the coexistence of the two detected phases.

In relation to the lattice parameters, it is noticed that the γ-$Al_2O_3$changes according to the temperature, while the α-$Al_2O_3$ shows no variation because it is considered stable.

The particles of the powders obtained in the three steps of phase transition can be viewed by means of images of transmission electronic microscopy (TEM) displayed in Figs. 1(c), 2(c) and 3(c).

Besides demonstrating the particles growth as function of the phase transition, it was possible to compare data of particles sizes obtained by BET, XRD and TEM (Table 2) and literature data [16].

Table 2 compares particle size data obtained by specific surface area using BET method (Eq. (1)), crystallite size calculated by Gaussian adjust of the XRD diffraction patterns and observation of TEM micrographs for alumina powders calcined at different temperatures. The results obtained are in accordance with previous works [1,5,16], in spite of the different preparation methods used by these authors.

Table 2 shows dependence of average particle size on the calcining temperature. From 700 ° C on, the particle size of the samples decreases with the increase of the calcining temperature, until the minimum value is reached at 900 °C. This is due to the crystallization of γ-phase, whose particles are typically ultrafine. As γ-$Al_2O_3$ changes to α-$Al_2O_3$, the particle size increases, which means that the gaps between the chains and the crystal defects are gradually reduced and finally disappear, accomplishing the crystallization of α-$Al_2O_3$ phase. Fig. 4 shows that crystallite size calculated from XRD diffraction patterns is closely related to γ-$Al_2O_3$ to α-$Al_2O_3$ phase transition.

At temperatures in which there are 100% of γ-$Al_2O_3$ (800–950 °C), the crystallite size is small (5–10 nm), having

Table 2
Particle size data (in nm) obtained by specific surface area ($d_{BET}$) using BET method (Eq. (1)), crystallite size ($d_{XRD}$) calculated by Gaussian adjust of the XRD diffraction patterns and observation of TEM micrographs for alumina powders calcined at different temperatures

| | Temperature (°C) | | | | | | | | |
|---|---|---|---|---|---|---|---|---|---|
| | 700 | 800 | 900 | 950 | 1000 | 1025 | 1050 | 1100 | 1200 |
| $d_{XRD}$ | | 8.9 | 6.7 | 7.0 | 22.0 | 59.5 | 62.5 | 64.2 | 66.2 |
| $d_{BET}$ | 133.8 | 43.5 | 34.5 | | 50.9 | | | 226.2 | |
| $d_{TEM}$ | | | | 10.0 | | 55.0 | 110.0 | | |

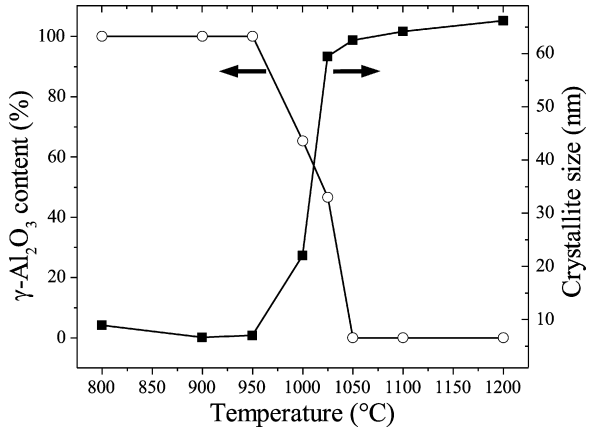


Fig. 4. Relationship between γ-$Al_2O_3$ to α-$Al_2O_3$ phase transition and crystallite size calculated from XRD diffraction patterns.

a growth in the temperature range in which the phase transition occurs (950–1050 °C), reaching about 60 nm for subsequent temperatures (1050–1200 °C) where all γ-$Al_2O_3$ is converted in α-$Al_2O_3$.

Similar increases in crystallite size accompanying the formation of α-$Al_2O_3$ have been reported for alumina powders prepared by other methods [16–18].

## 4. Conclusion

The steps of phase transition γ → α-$Al_2O_3$were in number of three when characterized by X-ray diffraction (XRD), micro-Raman spectroscopy and transmission electronic microscopy (TEM) techniques. In the first step, in the range 800–950 °C, the synthesized powder is constituted of γ-$Al_2O_3$ according to results presented in XRD patterns. In this step, the cubic symmetry of γ-$Al_2O_3$ structure (space group *Fd3m*) leads to a low signal of micro-Raman spectra with particle size about ∼ 10 nm, as observed in TEM micrographs. In the second step, in the range 1000–1025 °C, the occurrence of phase transition is indicated by the coexistence of two phases (γ + α-$Al_2O_3$) according to XRD patterns. Characteristic peaks of corundum symmetry (α-$Al_2O_3$, space group $R\bar{3}c$) appear in the micro-Ramam spectra and the TEM micrograph reveal the occurrence of both phases with average particle size of ∼ 55 nm. In the final step, above 1050 °C, the aluminum oxide appears completely converted into α-$Al_2O_3$, showing high crystallinity according to XRD patterns. Micro-Raman spectra present increase in the intensity of peaks due to corundum symmetry and the TEM micrographs are indicative to a growth of particle size above ∼ 100 nm. It can also be concluded that the crystallite size calculated by XRD results is closely related to the phase transition, i.e., crystallite size increases according to the phase transition variation and consequently, with the increase in temperature.

## Acknowledgments

The authors gratefully acknowledge the financial support of the Brazilian financing agencies FAPESP (proc. 00/12353-5)/ CEPID, CNPq (proc. 150330/2003-0) and Fundação Araucária.

## References


[1] H. Noda, K. Muramoto, H. Kim, Preparation of nano-structured ceramics using nanosized $Al_2O_3$ particles, J. Mater. Sci. 38 (2003) 2043–2047.

[2] P.A. Janeway, Nanotechnology—it's more than size, Am. Ceram. Soc. Bull. 82 (4) (2003) 31–38.

[3] S. Kim, J.J. Gislason, R.W. Morton, X.Q. Pan, H.P. Sun, R.M. Laine, Liquid-feed flame spray pyrolysis of nanopowders in the alumina-titania system, Chemi. Mater. 16 (12) (2004) 2336–2343.

[4] K.J. Rao, K. Mahesh, S. Kumar, A strategic approach for preparation of oxide nanomaterials, Bull. Mater. Sci. 28 (1) (2005) 19–24.

[5] R.K. Pati, J.C. Ray, P. Pramanik, A novel chemical route for the synthesis of nanocrystalline α-$Al_2O_3$, Mater. Lett. 44 (2000) 299–303.

[6] S. Cava, S.M. Tebcherani, S.A. Pianaro, C.A. Paskocimas, E. Longo, J. Varela, Structural and spectroscopic analysis of γ-$Al_2O_3$ to α-$Al_2O_3$–$CoAl_2O_4$ phase transition, Mater. Chem. Phys. 97 (2006) 102–108.

[7] B.H. Toby, EXPGUI, a graphical user interface for GSAS, J. Appl. Crystallogr. 34 (2001) 210–213.

[8] P. Thompson, D.E. Cox, J.B. Hastings, Rietveld refinement of debye-scherrer synchrotron X-ray data from $Al_2O_3$, J. Appl. Crystallogr. 20 (1987) 79–83.

[9] L.W. Finger, D.E. Cox, A.P. Jephcoat, A correction for powder diffraction peak asymmetry due to axial divergence, J. Appl. Crystallogr. 27 (1994) 892–900.

[10] P.W. Stephens, Phenomenological model of anisotropic peak broadening in powder diffraction, J. Appl. Crystallogr. 32 (1999) 281–289.

[11] G. Gutirrez, A. Taga, B. Johansson, Theoretical structure determination of γ-$Al_2O_3$, Phys. Rev. B 65 (012101) (2001) 1–4.

[12] R.J. Damani, P. Makroczy, Heat treatment induced phase and microstructural development in bulk plasma sprayed alumina, J. Eur. Ceram. Soc. 20 (2000) 867–888.

[13] C. Zuo, P.W. Jagodzinski, R-line luminescence from trace amounts of $Cr^{3+}$ in aluminium oxide and its dependence on sample hydration, Appl. Spectrosc. 56 (2002) 1055–1058.

[14] I.D. Brown, B. McMahon, CIF: the computer language of crystallography, Acta Crystallogr. Sect. B: Struct. Sci. 58 (2002) 317–324.

[15] S.R. Hall, F.H. Allen, I.D. Brown, The crystallographic information file (CIF)—a new standard archive file for crystallography, Acta Crystallogr. Sect. A 47 (1991) 655–685.

[16] P.L. Chang, F.S. Yen, K.C. Cheng, H.L. Wen, Examinations on critical and primary crystallite sizes during θ- to α-phase transformations of ultrafine alumina powders, Nano Lett. 1 (5) (2001) 253–261.

[17] J. Ding, T. Tsuzuki, P.G. McCormick, Ultrafine alumina particles prepared by mechanochemical/thermal processing, J. Am. Ceram. Soc. 79 (11) (1996) 2956–2958.

[18] T. Hirayama, High-temperature characteristics of transition $Al_2O_3$ powder with ultrafine spherical-particles, J. Am. Ceram. Soc. 70 (6) (1987) C-122.